High-Speed Combinatorial Polymerization through Kinetic-Trap Encoding

Félix Benoist and Pablo Sartori*
Gulbenkian Institute for Molecular Medicine, Oeiras, Portugal

(Received 12 August 2024; accepted 12 December 2024; published 23 January 2025)

Like the letters in the alphabet forming words, reusing components of a heterogeneous mixture is an efficient strategy for assembling a large number of target structures. Examples range from synthetic DNA origami to proteins self-assembling into complexes. The standard self-assembly paradigm views target structures as free-energy minima of a mixture. While this is an appealing picture, at high speed structures may be kinetically trapped in local minima, reducing self-assembly accuracy. How then can high speed, high accuracy, and combinatorial usage of components coexist? We propose to reconcile these three concepts not by avoiding kinetic traps, but by exploiting them to encode target structures. This can be achieved by sculpting the kinetic pathways of the mixture, instead of its free-energy landscape. We formalize these ideas in a minimal toy model, for which we analytically estimate the encoding capacity and kinetic characteristics, in agreement with simulations. Our results may be generalized to other soft-matter systems capable of computation, such as liquid mixtures or elastic networks, and pave the way for high-dimensional information processing far from equilibrium.

DOI: 10.1103/PhysRevLett.134.038402

Introduction—The combinatorial usage of different components is a prevalent biological strategy to encode information. For example, in the cytoplasm, proteins accurately self-assemble into complexes that share proteins with one another [1,2]. This notion has also permeated nanotechnology [3,4], where the same set of DNA tiles can be reused to reliably self-assemble multiple structures [5]. Besides reusability and high accuracy, a fundamental property of biological self-assembly is high speed, which allows cellular adaptation to quickly changing conditions. This motivates the fundamental question of how self-assembly with reusable components can occur quickly and accurately.

The standard approach to combinatorial self-assembly encodes target structures as minima of the mixture's free-energy landscape [6–8]. While never explicitly mentioned, this approach is subject to a speed-accuracy trade-off [9,10]: self-assembly of targets is accurate when the mixture can relax to target minima in near-equilibrium conditions. Far from equilibrium, as required for high speed, free-energy encoding results in undesired structures trapping the kinetics. To reconcile self-assembly speed, accuracy, and reusability we propose an alternative encoding approach: tuning the kinetics of the pathways leading to target structures. In this approach, kinetic traps, normally understood as deleterious [11–14], can be exploited to encode information that is accessible far from equilibrium and at high speed [15–18]. While tuning the kinetics of different binding partners is a well-established mechanism for discrimination in copolymerization processes [10,19], its role in self-assembly remains understudied.

In this Letter, we model the dynamics of a self-assembling heteropolymer in contact with a reservoir of

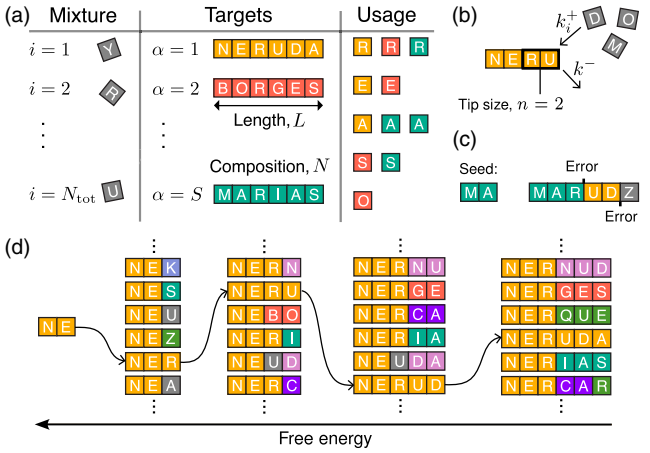

FIG. 1. Schematics of kinetic encoding setup. (a) A heterogeneous mixture of N_{tot} monomer species is designed to self-assemble S different target strings of size L and containing N different components, which results in combinatorial usage of components. (b) A polymer grows by adding or removing monomers at its tip with rates k_i^+ and k^- that depend on the composition of the n components of the polymer tip. (c) When multiple targets are encoded, different nucleation seeds should retrieve different targets. Retrieval is hampered by errors due to the reusability of components (first error) or thermal fluctuations (second error). (d) In kinetic encoding there is no free-energy difference between different strings of the same size. Instead, the pathway to the target is differentiated by kinetics.

*Contact author: pablo.sartori@gimm.pt

multiple different component species. We show how a large number of target strings can be encoded kinetically, such that accurate self-assembly of any of them will occur at high speed. Furthermore, we analytically calculate and numerically confirm the scaling of the maximum number of structures that a mixture can kinetically encode, the characteristic lifetime of targets, and the dependence of our results on the heterogeneity of targets and their usage of components.

Model setup—We consider a mixture of $N_{\rm tot}$ different monomer species; see Fig. 1(a), labeled $i = 1, \ldots, N_{\rm tot}$, that are kept at fixed chemical potentials, $\mu_i = \mu$, and temperature, T (hereafter $k_{\rm B}T = 1$, with $k_{\rm B}$ Boltzmann's constant). We are interested in conditions under which the mixture can self-assemble any of S different target strings, labeled $\alpha = 1, \ldots, S$, that are defined through composition vectors $\mathbf{c}^\alpha = \{i_1^\alpha, i_2^\alpha, \ldots, i_L^\alpha\}$, with L the length (equal for all targets). Each target contains $N \leq N_{\rm tot}$ different monomer species, and is thus characterized by its usage of the mixture, $u = N/N_{\rm tot} \leq 1$, and its compositional heterogeneity, $h = N/L \leq 1$. The reusability of components, within and across strings, allows for a combinatorial expansion of the mixture.

We study the dynamics of a heteropolymer that grows by adding and removing monomers of the mixture at its distal end; see Figs. 1(b)–1(d). The polymer in question is characterized by its composition vector $\{i_1, i_2, \ldots, i_\ell\}$, with ℓ the time-varying length. The addition and removal of monomers depends on the composition of the polymer tip, $\mathbf{t}_n = \{i_{\ell+1-n}, \ldots, i_\ell\}$, with $n \geq 1$ the length of the tip, i.e., the range of interactions. We denote the addition rate of a monomer from species i as $k_i^+(\mathbf{t}_n)$, and the removal rate of monomer i_ℓ as $k^-(\mathbf{t}_{n+1})$. Note that the case $n = 1$ corresponds to nearest-neighbor coupling among monomers, $n = 2$ to next-nearest-neighbor, etc. Within this setup, our goal is to propose a choice of rates that allows polymerization of target strings reliably and fast.

To ensure fast retrieval of targets, we encode their compositions in the binding kinetics, rather than in the energetics, of the mixture components. Therefore, considering the binding of component i to a tip $\mathbf{t}_n$ and its subsequent unbinding (from a tip $\mathbf{t}'_{n+1}$ corresponding to the previous tip $\mathbf{t}_n$ to which has been added i), the detailed balance condition on the rates reduces to

$$k_i^+(\mathbf{t}_n)/k^-(\mathbf{t}'_{n+1}) = \exp(\mu), \tag{1}$$

which encodes no information about the targets. The targets are instead kinetically encoded through the choice of forward rates,

$$k_i^+(\mathbf{t}_n) = \exp(r_i\delta), \tag{2}$$

where r_i is the number of monomers in the tip $\mathbf{t}_n$ that are correctly placed relative to monomer i at location $\ell + 1$ in any target string $\mathbf{c}^\alpha$ (see [20] for explicit formula), and δ is a kinetic discrimination parameter. Note that the rates are defined up to an irrelevant time unit. As an illustration, for the simple case $n = 1$ this rule implies that $r_i = 1$ if the monomer i to be added is a neighbor of the tip monomer i_ℓ in any of the target strings, and $r_i = 0$ otherwise. Alternatively, in the example of Fig. 1(b) with $n = 2$, we have $k_{\rm D}^+(\{\mathrm{R},\mathrm{U}\}) = \exp(2\delta)$ due to the target $\mathbf{c}^1 = \{\mathrm{N},\mathrm{E},\mathrm{R},\mathrm{U},\mathrm{D},\mathrm{A}\}$, but $k_{\rm Z}^+(\{\mathrm{R},\mathrm{U}\}) = 1$. In the following, we study the conditions under which this minimal model allows accurate and fast retrieval of targets.

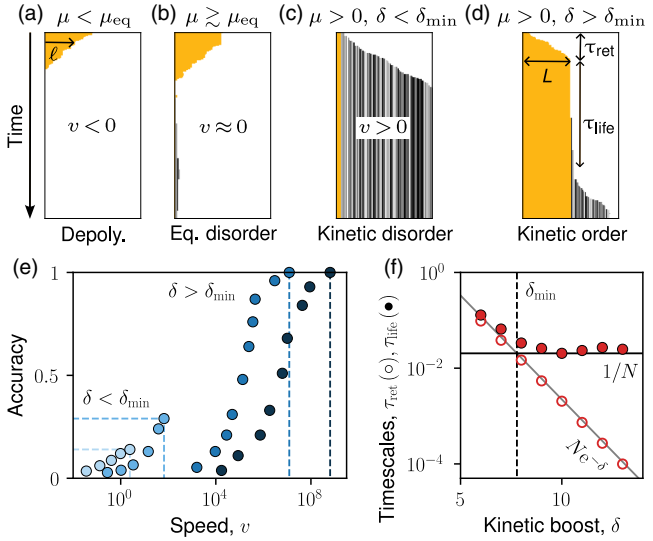

FIG. 2. Fast and accurate retrieval of a single target string. (a)–(d) Kymographs of polymer dynamics obtained from stochastic simulations (white codes for empty sites, yellow for components matching the target string, and shades of gray assembly errors); see [20] for simulation details. In this and all panels the mixture encodes a single target ($S = 1$) that is heterogeneous and uses all components ($L = N_{\rm tot} = N = 50$). The polymer tip size is $n = 1$ (nearest-neighbor coupling). Depending on the chemical potential (μ) and discrimination barrier (δ) we identify four different kinetic regimes. (e) As μ increases, both the accuracy of target retrieval and the speed increase. The maximal accuracy and maximal speed (dashed lines) for $\mu \to \infty$ both increase with δ. In particular, the accuracy approaches one for $\delta > \delta_{\rm min}$ [Eq. (3)]. Here, $n = 2$ and shades of blue label $\delta = \{4, 6, 12, 14\}$ by increasing darkness. (f) The timescale of target retrieval ($\tau_{\rm ret}$) and the lifetime of a target ($\tau_{\rm life}$) separate for $\delta > \delta_{\rm min}$, in quantitative agreement with Eq. (4). Here again $n = 1$.

Retrieving a target string as a kinetic trap—As a starting point, we consider that the mixture encodes a single string ($S = 1$) that is fully heterogeneous ($h = 1$) and uses all components ($u = 1$, such that $L = N_{\rm tot} = N$). In this case, errors are not due to combinatorial usage of components [first error in Fig. 1(c)], but instead emerge from thermal fluctuations [second error in Fig. 1(c)]. At equilibrium, the chemical potential of the mixture balances the entropic tendency to grow, and so $\mu_{\rm eq} = -\ln N < 0$ [9,10,21]. Equation (1) implies that no information is encoded in

the binding energies, and so the equilibrium state of the polymer is fully disordered: for $\mu \gtrsim \mu_{\rm eq}$ an initially ordered seed will disassemble in favor of a disordered polymer [Fig. 2(b)]. This equilibrium state defines a boundary between a depolymerization regime, where the growth speed v (defined as the net rate of monomer addition) is negative, i.e., $v < 0$ for $\mu < \mu_{\rm eq}$ [Fig. 2(a)], and different growth regimes, for which $\mu > \mu_{\rm eq}$ implies $v > 0$ [Figs. 2(c) and 2(d)].

Equation (2) establishes that target strings are encoded in the kinetics, instead of the energetics. Therefore, the accuracy of retrieval should be maximal when the dynamics are strongly irreversible [10]. Since in accurate and irreversible dynamics there is only one possible assembly pathway, the bound on the driving is raised to $\mu > 0$. Furthermore, suppressing errors due to the presence of $N-1$ confounding monomers at each growth step requires that the kinetic discrimination barrier, δ, be sufficiently large.

To bound δ, we estimate the error rate $p_{\rm err}$ as the ratio of the sum of addition rates for all potential erroneous additions to the addition rate of the correct monomer, i.e., $p_{\rm err} \approx (N-1)/\exp(n\delta)$. In the highly irreversible regime, the probability to retrieve the seeded target can be estimated as $(1-p_{\rm err})^N$. For $N \gg 1$, a significant retrieval probability thus requires $N p_{\rm err} \ll 1$. This leads to a lower bound on the kinetic discrimination parameter

$$\delta_{\rm min} = \frac{2}{n} \ln N. \tag{3}$$

We distinguish two fast-growth regimes: kinetic disorder for $\delta < \delta_{\rm min}$, in which thermal fluctuations result in frequent addition errors, i.e., $p_{\rm err} \approx 1$ [Fig. 2(c)]; and kinetic order for $\delta > \delta_{\rm min}$, in which a target string is accurately retrieved, i.e., $p_{\rm err} \approx 0$, until a fluctuation destabilizes it [Fig. 2(d)].

Figure 2(e) shows that increasing the driving μ results in an increase of the growth speed, up to saturation at $v \approx \exp(n\delta)$, as well as an increase in retrieval accuracy (defined as the fraction of string length assembled until the first error). Still, high accuracy is only possible for large discrimination barriers, in agreement with Eq. (3).

Kinetic encoding implies that targets are not thermodynamically stable. We can however estimate their kinetic stability. The time it takes to retrieve a target string, $\tau_{\rm ret}$, is obtained by dividing the length of the string, N, by its growth speed, v, and so $\tau_{\rm ret} \approx N \exp(-n\delta)$. In contrast, the lifetime of the string, $\tau_{\rm life}$, is given by the time it takes to add a few incorrect monomers, and so $\tau_{\rm life} \approx 1/N$. Therefore, the lifetime of a string relative to its retrieval time reads

$$\tau_{\rm life}/\tau_{\rm ret} \approx \exp(n\delta)/N^2, \tag{4}$$

and so larger discrimination barriers and longer tip sizes result in more stable strings; see Fig. 2(f). To conclude, we have shown that the kinetic encoding approach in Eq. (2) allows for fast and accurate retrieval of a single target string for strong discrimination far from equilibrium.

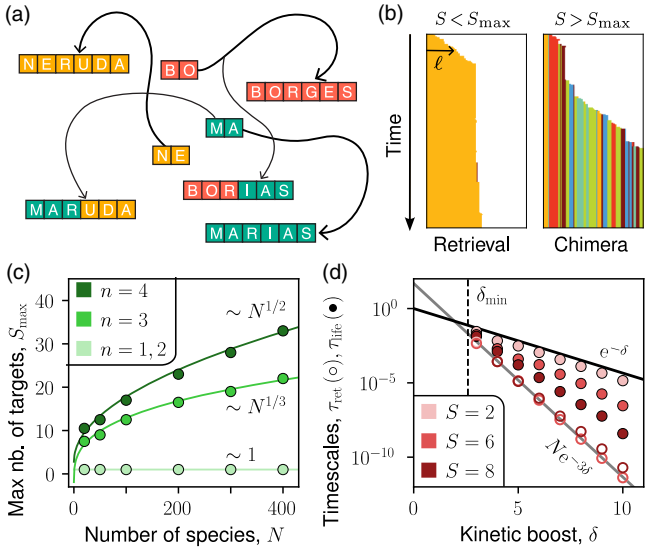

FIG. 3. Combinatorial encoding of kinetic pathways. (a) Reusing components across targets strings can result in chimeric assemblies, as kinetic pathways will interfere (a kinetic analogy of crosstalk of multiple minima). (b) To avoid chimeric strings, the number of target strings S must be smaller than $S_{\rm max}$ [Eq. (5)]. Here, $S_{\rm max} \approx 3$, and the two values of S are 2 and 6. Throughout this figure we used $N = L = N_{\rm tot} = 50$ and $\mu = 3$. In this panel, $\delta = 5$ and $n = 2$. (c) The capacity limit increases with the target size N depending on the monomer connectivity n according to Eq. (5). (d) Target stability deteriorates with increasing number of target strings S. Here, $n = 3$, such that $S_{\rm max} = 9$.

Combinatorial encoding far from equilibrium—We now turn to the case in which the mixture encodes multiple targets ($S > 1$) by combinatorially reusing components across targets [6,8]. In this scenario, errors arise when one component has as neighbors two different components in two different targets, making these two targets indistinguishable to the tip of a growing polymer. For example, in Fig. 1(c) for the state {M,A,R} of the polymer and $n = 1$ we have that $k_{\rm I}^+ = k_{\rm U}^+ = \exp(\delta)$, due to {R} appearing both in $\mathbf{c}^1 = \{\mathrm{N,E,R,U,D,A}\}$ and $\mathbf{c}^S = \{\mathrm{M,A,R,I,A,S}\}$, which can result in the error shown. Such types of errors cannot be suppressed by increasing δ. Conceptually, if the mixture encodes many kinetic pathways to different targets, such pathways may cross, making it likely to retrieve a chimera (formed by fragments of different target strings) rather than the seeded target string [Fig. 3(a)]. In Fig. 3(b), we show two examples of successful and failed retrieval for a mixture that kinetically encodes multiple target strings. For the same large positive values of μ and δ, if the number of stored targets is below a certain maximal value, $S < S_{\rm max}$, retrieval is successful; instead if $S > S_{\rm max}$, the initial seed nucleates fragments from many other different target strings, yielding a chimeric polymer [6,8].

What determines the maximum number of target strings, $S_{\max}$, that can be accurately assembled from a mixture via kinetic encoding? To answer this question, we define the promiscuity of components, π, as the number of specific interactions of a typical component at each nearest-neighboring location. For instance, for the targets shown in Fig. 1(a), monomer {R} interacts with $\pi = 3$ different monomer species at each nearest-neighbor location. A large promiscuity turns components indistinguishable, irrespective of δ, hampering the reliability of assembly. The error rate, p_{err}, thus corresponds to the probability that given a tip of size n there is ambiguity regarding which component can be added. For $n = 1$, we estimate $p_{\mathrm{err}} \approx (\pi - 1)/\pi$, whereas for $n \geq 2$, the error rate scales as $p_{\mathrm{err}} \sim (\pi - 1)^n/N^{n-1}$ (see [20] for derivation). We then impose the condition $Np_{\mathrm{err}} \ll 1$, as in the derivation of Eq. (3), focusing on the case where all components are used once in every target ($h = u = 1$), for which $\pi \approx S$. This yields $S_{\max} = 1$ for $n = 1$, because the error rate, $p_{\mathrm{err}} \approx (S - 1)/S$, prevents retrieval of as little as two targets. For the case $n \geq 2$, we obtain

$$S_{\max} \sim N^{1-2/n}. \tag{5}$$

The predicted size scaling goes from $\mathcal{O}(1)$ for $n = 2$, and thus no combinatorial usage is possible, to $\mathcal{O}(N)$ for the fully connected case $n = N$, akin to neural network capacity [22]. Therefore, increasing the tip size improves discrimination, which allows to encode more targets.

Figure 3(c) shows the results of numerical simulations relating the capacity, $S_{\max}$, to the number of component species, N, for different tip sizes, n. As one can see, for $n = 1, 2$ no combinatorial usage of components is possible, whereas for $n = 3$, 4 the numerical results are in good agreement with the predictions of Eq. (5). Figure 3(d) shows how the time of retrieval, τ_{ret}, and lifetime, τ_{life}, depend on the kinetic discrimination parameter δ for different numbers of target strings, S. While τ_{ret} follows the behavior derived earlier, τ_{life} is now bounded by $\exp(-\delta)$, because errors are dominated by component reusability. As S increases, τ_{life} decreases, making structures more unstable as S approaches the capacity limit, $S_{\max}$. Overall, we conclude that kinetic encoding of a combinatorially large number of components is possible, with a capacity and stability that agree with our analytical estimates.

The roles of heterogeneity and usage—We now study the effect of target heterogeneity, h, and usage of components, u, on the capacity of the system, $S_{\max}$. In this general case, the promiscuity of components is given by $\pi \approx Su/h$ for large heterogeneous targets [20]. Following an argument analogous to the previous section, i.e., $Lp_{\mathrm{err}} \ll 1$ with $p_{\mathrm{err}} \sim (\pi - 1)^n/N_{\mathrm{tot}}^{n-1}$, the scaling in Eq. (5) generalizes to

$$S_{\max} \sim (h/u)^{2-1/n} L^{1-2/n}, \tag{6}$$

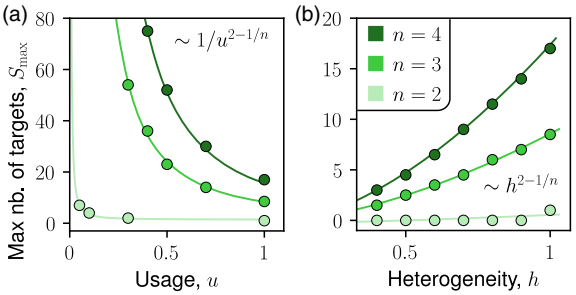

FIG. 4. Effects of component usage and heterogeneity in combinatorial encoding. (a) The maximum capacity, $S_{\max}$, decreases with increasing usage, u, at fixed length L as predicted by Eq. (6). (b) $S_{\max}$ increases with increasing heterogeneity, h, also in quantitative agreement with Eq. (6). In both panels, $L = 25$ for $n = 2$, and $L = 100$ for $n = 3$, 4.

for $n \geq 2$. This expression highlights the role of the target string length L as a key extensive quantity regulating the scaling. Equation (6) also shows that increasing heterogeneity and reducing usage both result in an increase of the capacity. The intuition behind this is simple. Increasing heterogeneity will reduce the reusability of components within each target. Likewise, reducing the usage of components made by each target string reduces the reusability across targets. Both aspects reduce the promiscuity of components, thus facilitating that polymerization pathways of different targets stay separate from each other. Figure 4 shows that our numerical simulations recover the capacity scaling in Eq. (6). In particular the capacity diverges as the usage becomes low ($u \to 0$), and reaches a maximum for fully heterogeneous structures ($h = 1$). Therefore, high heterogeneity and low usage of available components results in increased capacity for kinetic encoding, as dictated by Eq. (6).

Discussion—Classical self-assembly relies on the stability of target structures, which results in a trade-off between self-assembly speed and accuracy. In contrast, combining ideas of information thermodynamics [9,10,23] and neuroscience [22,24], we have shown how self-assembly of heterogeneous target structures can be performed kinetically. In this approach, higher speed implies higher accuracy, breaking the aforementioned trade-off [25,26]. Since assemblies in this scenario do not correspond to deep energy minima, but to long-lived kinetic traps, they are only stable for a finite amount of time.

The concept of kinetic encoding of target structures is motivated by the self-assembly of large heteromeric protein complexes, such as the ribosome [27]. It is well established that specific binding events for these systems are catalyzed by enzymes lowering the kinetic barrier for binding [28,29]. The importance of such enzymes, often referred to as assembly factors, cannot be understated, as their deletion results in the slowdown of the self-assembly speed and the accumulation of incomplete structures [28,30]. In

fact, there are often as many assembly factors as components in a given assembly [29,31,32]. In this sense, our choice of binding rates can be understood as coarse-graining enzymatic reactions due to assembly factors. More broadly, both kinetic encoding (as studied here) and energetic encoding (see Refs. [6–8]) are expected to play a role. How best to combine them for maximal efficiency remains an open question; see [20] for additional discussion details (and Refs. [33–38] therein).

While we have illustrated the concept of kinetic-trap encoding in a toy model of heteromeric polymerization, this idea may be adaptable to systems in other branches of soft-matter physics, which at present all use energetic interactions to encode target functions. Examples include self-assembly of structures with more complex geometries [39,40], programmable liquid phases [41,42], colloidal self-assembly [43,44], guided self-folding [3,45], or elastic network models of proteins [46,47]. Since the biophysical systems that these models aim to describe often operate far from equilibrium, we expect the generic features of kinetic encoding here presented will play a central role in explaining how biological matter is capable of complex high-dimensional information processing.

Acknowledgments—This work was partly supported by a laCaixa Foundation grant (LCF/BQ/PI21/11830032) and core funding from the Gulbenkian Foundation.

[1] A.-C. Gavin *et al.*, Proteome survey reveals modularity of the yeast cell machinery, Nature (London) **440**, 631 (2006).
[2] S. Kühner *et al.*, Proteome organization in a genome-reduced bacterium, Science **326**, 1235 (2009).
[3] K. E. Dunn, F. Dannenberg, T. E. Ouldridge, M. Kwiatkowska, A. J. Turberfield, and J. Bath, Guiding the folding pathway of DNA origami, Nature (London) **525**, 82 (2015).
[4] W. Meng, R. A. Muscat, M. L. McKee, P. J. Milnes, A. H. El-Sagheer, J. Bath, B. G. Davis, T. Brown, R. K. O'Reilly, and A. J. Turberfield, An autonomous molecular assembler for programmable chemical synthesis, Nat. Chem. **8**, 542 (2016).
[5] C. G. Evans, J. O'Brien, E. Winfree, and A. Murugan, Pattern recognition in the nucleation kinetics of non-equilibrium self-assembly, Nature (London) **625**, 500 (2024).
[6] A. Murugan, Z. Zeravcic, M. P. Brenner, and S. Leibler, Multifarious assembly mixtures: Systems allowing retrieval of diverse stored structures, Proc. Natl. Acad. Sci. U.S.A. **112**, 54 (2015).
[7] G. Bisker and J. L. England, Nonequilibrium associative retrieval of multiple stored self-assembly targets, Proc. Natl. Acad. Sci. U.S.A. **115**, E10531 (2018).
[8] P. Sartori and S. Leibler, Lessons from equilibrium statistical physics regarding the assembly of protein complexes, Proc. Natl. Acad. Sci. U.S.A. **117**, 114 (2020).
[9] C. H. Bennett, Dissipation-error tradeoff in proofreading, BioSystems **11**, 85 (1979).
[10] P. Sartori and S. Pigolotti, Kinetic versus energetic discrimination in biological copying, Phys. Rev. Lett. **110**, 188101 (2013).
[11] F. M. Gartner, I. R. Graf, and E. Frey, The time complexity of self-assembly, Proc. Natl. Acad. Sci. U.S.A. **119**, e2116373119 (2022).
[12] Z. Jia, J. D. Schmit, and J. Chen, Amyloid assembly is dominated by misregistered kinetic traps on an unbiased energy landscape, Proc. Natl. Acad. Sci. U.S.A. **117**, 10322 (2020).
[13] E. Sanz, C. Valeriani, D. Frenkel, and M. Dijkstra, Evidence for out-of-equilibrium crystal nucleation in suspensions of oppositely charged colloids, Phys. Rev. Lett. **99**, 055501 (2007).
[14] S. Osat, J. Metson, M. Kardar, and R. Golestanian, Escaping kinetic traps using nonreciprocal interactions, Phys. Rev. Lett. **133**, 028301 (2024).
[15] K. A. Dill and H. S. Chan, From levinthal to pathways to funnels, Nat. Struct. Biol. **4**, 10 (1997).
[16] A. Murugan, J. Zou, and M. P. Brenner, Undesired usage and the robust self-assembly of heterogeneous structures, Nat. Commun. **6**, 6203 (2015).
[17] B. Lefebvre and C. Maes, Frenetic steering in a non-equilibrium graph, J. Stat. Phys. **190**, 90 (2023).
[18] S. Whitelam, R. Schulman, and L. Hedges, Self-assembly of multicomponent structures in and out of equilibrium, Phys. Rev. Lett. **109**, 265506 (2012).
[19] Y.-C. Tsai and K. A. Johnson, A new paradigm for DNA polymerase specificity, Biochemistry **45**, 9675 (2006).
[20] See Supplemental Material at http://link.aps.org/supplemental/10.1103/PhysRevLett.134.038402 for additional details.
[21] D. Andrieux and P. Gaspard, Nonequilibrium generation of information in copolymerization processes, Proc. Natl. Acad. Sci. U.S.A. **105**, 9516 (2008).
[22] J. J. Hopfield, Neural networks and physical systems with emergent collective computational abilities, Proc. Natl. Acad. Sci. U.S.A. **79**, 2554 (1982).
[23] C. H. Bennett, The thermodynamics of computation—a review, Int. J. Theor. Phys. **21**, 905 (1982).
[24] J. Hertz, A. Krogh, and R. G. Palmer, *Introduction to the Theory of Neural Computation*, Santa Fe Institute Series (CRC Press, Boca Raton, 1991).
[25] S. Pigolotti and P. Sartori, Protocols for copying and proofreading in template-assisted polymerization, J. Stat. Phys. **162**, 1167 (2016).
[26] K. Banerjee, A. B. Kolomeisky, and O. A. Igoshin, Elucidating interplay of speed and accuracy in biological error correction, Proc. Natl. Acad. Sci. U.S.A. **114**, 5183 (2017).
[27] S. Klinge and J. L. Woolford, Ribosome assembly coming into focus, Nat. Rev. Mol. Cell Biol. **20**, 116 (2019).
[28] J. H. Davis and J. R. Williamson, Structure and dynamics of bacterial ribosome biogenesis, Phil. Trans. R. Soc. B **372**, 20160181 (2017).
[29] K. Dörner, C. Ruggeri, I. Zemp, and U. Kutay, Ribosome biogenesis factors—from names to functions, EMBO J. **42**, e112699 (2023).

[30] A. Seffouh, R. Nikolay, and J. Ortega, Critical steps in the assembly process of the bacterial 50s ribosomal subunit, Nucleic Acids Res. **52**, 4111 (2024).
[31] M. C. Wahl, C. L. Will, and R. Lührmann, The spliceosome: Design principles of a dynamic RNP machine, Cell **136**, 701 (2009).
[32] I. Vercellino and L. A. Sazanov, The assembly, regulation and function of the mitochondrial respiratory chain, Nat. Rev. Mol. Cell Biol. **23**, 141 (2022).
[33] M. A. Fox and J. K. Whitesell, *Organic Chemistry* (Jones & Bartlett Learning, 2004).
[34] M. Numata, S. Yagai, and T. Hamura, *Kinetic Control in Synthesis and Self-Assembly* (Academic Press, New York, 2018).
[35] M. Johansson, E. Bouakaz, M. Lovmar, and M. Ehrenberg, The kinetics of ribosomal peptidyl transfer revisited, Mol. Cell **30**, 589 (2008).
[36] K. B. Gromadski and M. V. R. Rodnina, Kinetic determinants of high-fidelity tRNA discrimination on the ribosome, Mol. Cell **13**, 191 (2004).
[37] M. T. Laub and M. Goulian, Specificity in two-component signal transduction pathways, Annu. Rev. Genet. **41**, 121 (2007).
[38] B. Alberts, A. Johnson, J. Lewis, D. Morgan, M. Raff, K. Roberts, and P. Walter, *Molecular Biology of the Cell*, 6th ed. (Garland Science, 2015).
[39] M. Lenz and T. Witten, Geometrical frustration yields fibre formation in self-assembly, Nat. Phys. **13**, 1100 (2017).
[40] B. Tyukodi, F. Mohajerani, D. M. Hall, G. M. Grason, and M. F. Hagan, Thermodynamic size control in curvature-frustrated tubules: Self-limitation with open boundaries, ACS Nano **16**, 9077 (2022).
[41] R. B. Teixeira, G. Carugno, I. Neri, and P. Sartori, Liquid hopfield model: Retrieval and localization in multi-component liquid mixtures, Proc. Natl. Acad. Sci. U.S.A. **121**, e2320504121 (2024).
[42] D. Zwicker and L. Laan, Evolved interactions stabilize many coexisting phases in multicomponent liquids, Proc. Natl. Acad. Sci. U.S.A. **119**, e2201250119 (2022).
[43] A. McMullen, M. Muñoz Basagoiti, Z. Zeravcic, and J. Brujic, Self-assembly of emulsion droplets through programmable folding, Nature (London) **610**, 502 (2022).
[44] F. Romano, J. Russo, L. Kroc, and P. Šulc, Designing patchy interactions to self-assemble arbitrary structures, Phys. Rev. Lett. **125**, 118003 (2020).
[45] D. E. P. Pinto, N. A. M. Araújo, P. Šulc, and J. Russo, Inverse design of self-folding 3d shells, Phys. Rev. Lett. **132**, 118201 (2024).
[46] L. Yan, R. Ravasio, C. Brito, and M. Wyart, Architecture and coevolution of allosteric materials, Proc. Natl. Acad. Sci. U.S.A. **114**, 2526 (2017).
[47] J. W. Rocks, N. Pashine, I. Bischofberger, C. P. Goodrich, A. J. Liu, and S. R. Nagel, Designing allostery-inspired response in mechanical networks, Proc. Natl. Acad. Sci. U.S.A. **114**, 2520 (2017).